Received:
4 June 2018
Revised:
12 September 2018
Accepted:
14 December 2018

Cite as: Fiona Hey, Catherine Andreadi, Catherine Noble, Bipin Patel, Hong Jin, Tamihiro Kamata, Kees Straatman, Jinli Luo, Kathryn Balmanno, David T. W. Jones, V. Peter Collins, Simon J. Cook, Christopher J. Caunt, Catrin Pritchard. Over-expressed, N-terminally truncated BRAF is detected in the nucleus of cells with nuclear phosphorylated MEK and ERK.
Heliyon 4 (2018) e01065.
doi: 10.1016/j.heliyon.2018.e01065

O - , - n h n c i c n h n g a c h h n g h h n

i ,[1] h n n i ,[1], h n ,[1], i n ,[1], n n , i , n [c], n i a , h n n , i . . n , . , h i h . g ,[2], n ich ,[*]

[a] Department of Molecular Cell Biology, University of Leicester, Lancaster Road, Leicester LE1 9HN, UK

[b] Leicester Cancer Research Centre, Clinical Sciences Building, University of Leicester, Leicester Royal Infirmary, Leicester LE2 7LX, UK

[c] Core Biotechnology Services, University of Leicester, Lancaster Road, Leicester LE1 9HN, UK

[d] Signalling Laboratory, The BabrahamBabraham Research ampuhes, ambridgheCB2E2 3ATX, UK

^{V600E}BRAF, although structural rearrangements, which remove N-terminal regulatory sequences, have also been reported. RAF-MEK-ERK signalling is normally thought to occur in the cytoplasm of the cell. However, in an investigation of BRAF localisation

[ec]ambridgheCB2f UK

using fluorescence microscopy combined with subcellular fractionation of Green

been detected at spindle poles and kinetochores in mitotic HeLa cells and knock-down of BRAF using siRNA resulted in early exit of cells from mitosis, perturbation of Mps1 localisation and the formation of pleiotropic spindle abnormalities and mis-aligned chromosomes [30]. BRAF isoforms have also been detected in nuclear fractions of the rat forebrain and cerebellum [31] with a recent investigation identifying BRAF in the nucleus of skeletal muscle cells after activation, where it was found to interact with and phosphorylate PAX3 leading to enhancement of MET activity, a requirement for limb muscle precursor cell migration [32]. However, the relevance of these alternative locations for BRAF and their role in downstream MEK/ERK signaling and BRAF-driven oncogenesis has not been fully explored as yet.

In this study, we have used tagged, exogenously expressed RAF proteins in NIH3T3 cells combined with fluorescence microscopy and fractionation methods to evaluate BRAF compartmentalisation in more detail. Surprisingly, we detect the accumulation of N-terminally truncated forms of BRAF in the nucleus whereas full length, wild-type BRAF and ^{V600E}BRAF are detected in the nucleus to a lower extent. Here, we correlate the compartmentalisation of these GFP-tagged forms of BRAF with the localisation of MEK and ERK in NIH3T3 cells.

2. [illegible]

2.1. c

To generate GFP-RAF expression vectors, cDNAs expressing wild-type or mutant versions of BRAF or CRAF were cloned into pEGFP-C1 vector (Clontech). GFP-ΔBRAF contains residues 449-804 of mouse BRAF, GFP-ΔCRAF contains residues 306-648 of human CRAF, GFP-FL-^{WT}BRAF contains residues 1-766 of human BRAF and GFP-FL-^{V600E}BRAF contains residues 1-766 of human BRAF with the V600E mutation. The human KIAA1549:BRAF and human ^{WT}BRAF cDNAs cloned within the pcDNA3.1 expression vector have been reported previously [33]. Mutations within GFP-ΔBRAF or GFP-FL-^{WT}BRAF were generated by performing site-directed mutagenesis using the GeneTailor^{TM} system (Thermo Fisher, 12397). Adenoviruses expressing human GFP-FL-^{WT}BRAF or human GFP-Δ

defined by the DAPI stain). Fluorescence measures were reported in arbitrary fluorescence units (AFU). To test for a positive correlation between nuclear PP-ERK/PP-MEK and nuclear GFP, cells were sorted into bins according to the nuclear GFP stain (each bin spanning 50−100 AFU) and, for each bin, the mean GFP value was plotted against the mean PP-ERK/PP-MEK stain intensity in the binned cells.

2. . i d ר ק ר i

Comparison between two groups was performed by the unpaired t test with Welch′s correction using Prism software version 7. The data are presented as the mean value and the error bars indicate ±SD or ±SEM (as indicated). Significance is indicated as *** for $p < 0.001$, ** for $p < 0.01$, * for $p < 0.05$ and not significant (NS) for p values > 0.05. For HCM, correlation coefficients were determined and compared us-

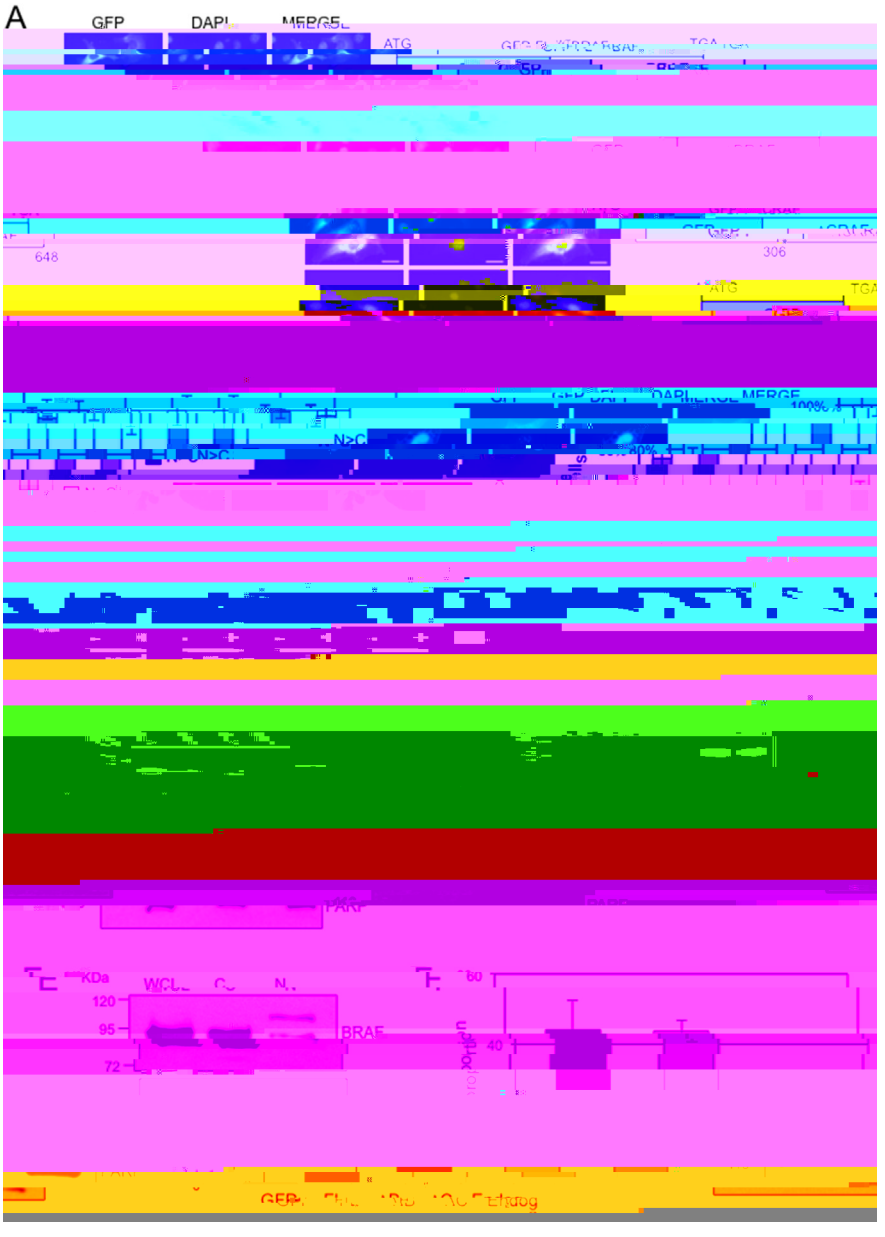

i . 1.

compartmentalisation by this method with a mean value of 44%. Quantitation of western blots, also generated a mean value of 18% for compartmentalisation of endogenous BRAF in the nucleus of NIH3T3 cells (Fig. 1F).

GFP fusion is used extensively as a method to study protein compartmentalisation and subcellular localisation. The main problem for nuclear localisation studies

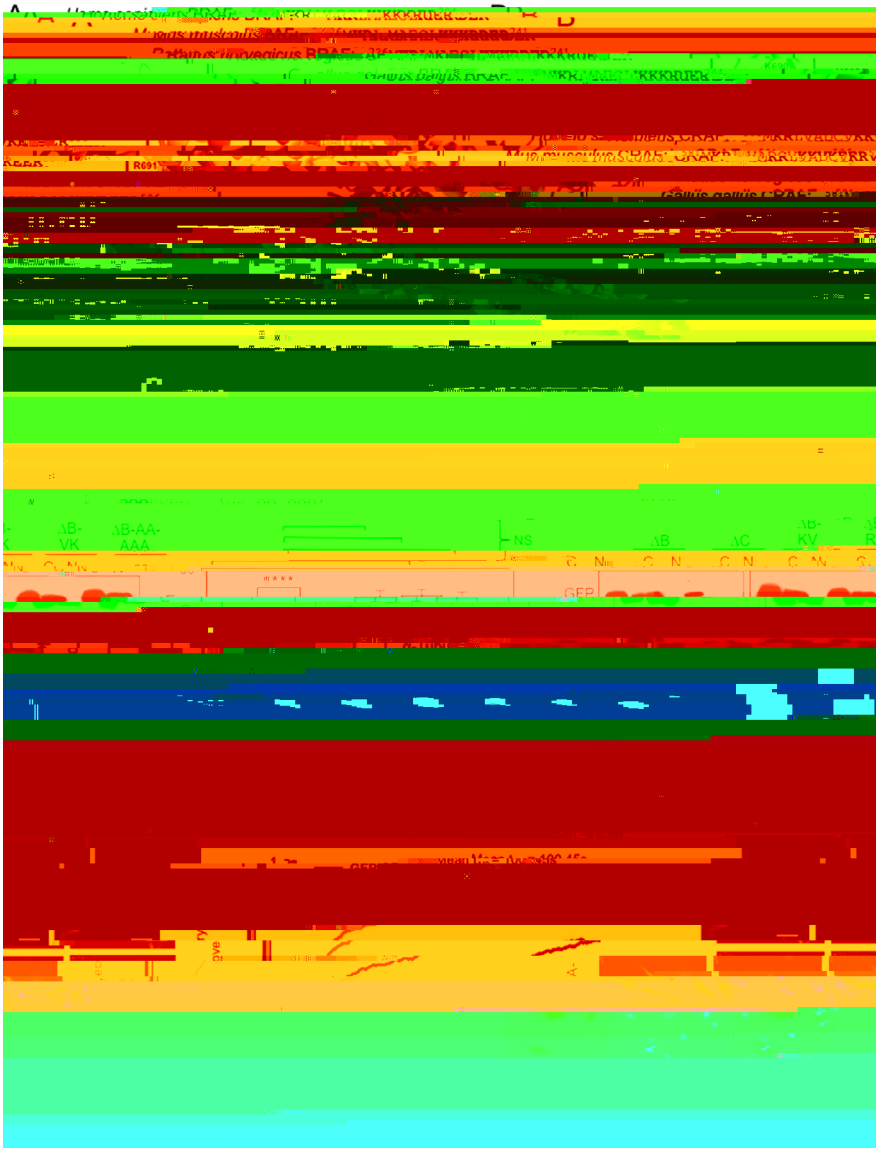

i . . GFP-ΔBRAF nuclear import is independent of a classical NLS. (A) Comparison of the amino acid sequences of a putative bipartite NLS within BRAF and RAF homologues from the indicated species. Sequences were taken from Ensembl (www.ensembl.org/index.html). (B) Ribbon diagram of the putative bipartite NLS within human BRAF. Expanded views of the exposed motifs at basic residues 690-691 (top expanded view) and 698-704 (bottom expanded view) are shown. (C) Mutation of the putative bipartite NLS in GFP-ΔBRAF. Four different mutants were generated within the putative NLS sequence at residues 726-741 of GFP-ΔBRAF. These vectors, along with GFP-ΔBRAF and GFP-ΔCRAF were transfected into NIH3T3 cells and nuclear and cytoplasmic fractions prepared. Western blots were analysed with the antibodies indicated. Western blot data were quantified using Image J analysis to generate the N:C proportion for the fusion proteins indicated in the bar chart on the right. Data represent mean ± SEM (GFP-ΔBRAF, n = 10; GFP-ΔCRAF, n = 4; all mutants, n = 3). The quantitative data for GFP-ΔBRAF and GFP-ΔCRAF are the same as that shown in Fig. 1F. (D) Representative fluorescence microscopy images of GFP-ΔBRAF and GFP-ΔBRAF carrying the AA-AAA mutations. Scale bars, 50 μm. (E) FRAP analysis of GFP-ΔBRAF. NIH3T3 cells transfected with vectors expressing either GFP-ΔBRAF

compartmentalisation of GFP-FL-^{WT}BRAF or GFP-ΔBRAF following expression in Craf knockout MEFs (Fig. 5A) while, in Araf knockout MEFs, there was a small but significant decrease in nuclear compartmentalisation of both fusion proteins (Fig. 5B). However, overall, these data identify no role for heterodimerisation in the tethering of the full-length protein in the cytoplasm.

We also examined a role of RAS by expressing GFP-FL-^{WT}BRAF and GFP-ΔBRAF in MEFs expressing oncogenic ^{G12D}KRAS and found that there was no significant difference in compartmentalisation compared to wild-type MEFs (Fig. 5C). Consistently, there was no significant difference in the compartmentalisation of GFP-FL-^{R188L}BRAF, which bears a mutation preventing RAS binding as assessed by both fluorescence microscopy (Fig. 5D) and fractionation (Fig. 5E). Creation of mutations in the 14-3-3 binding residue at S729A in GFP-FL-BRAF showed a small but significant increase in nuclear compartmentalisation as assessed by fluorescence microscopy (Fig. 5D) but this was not validated by fractionation (Fig. 5E). There was also no significant difference with respect to mutation of the S365 14-3-3 binding site (Fig. 5D, E).

It should be noted that, throughout our experiments, we observed some variability in the level of nuclear/cytoplasmic compartmentalisation of both GFP-FL-^{WT}BRAF and GFP-ΔBRAF in NIH3T3 cells (Fig. 1B) compared to the wild-type MEFs used in Fig. 5. We compared the 326-521 of chs-224119(mre)-326.5(except-224115for)-323.4(sil)-8

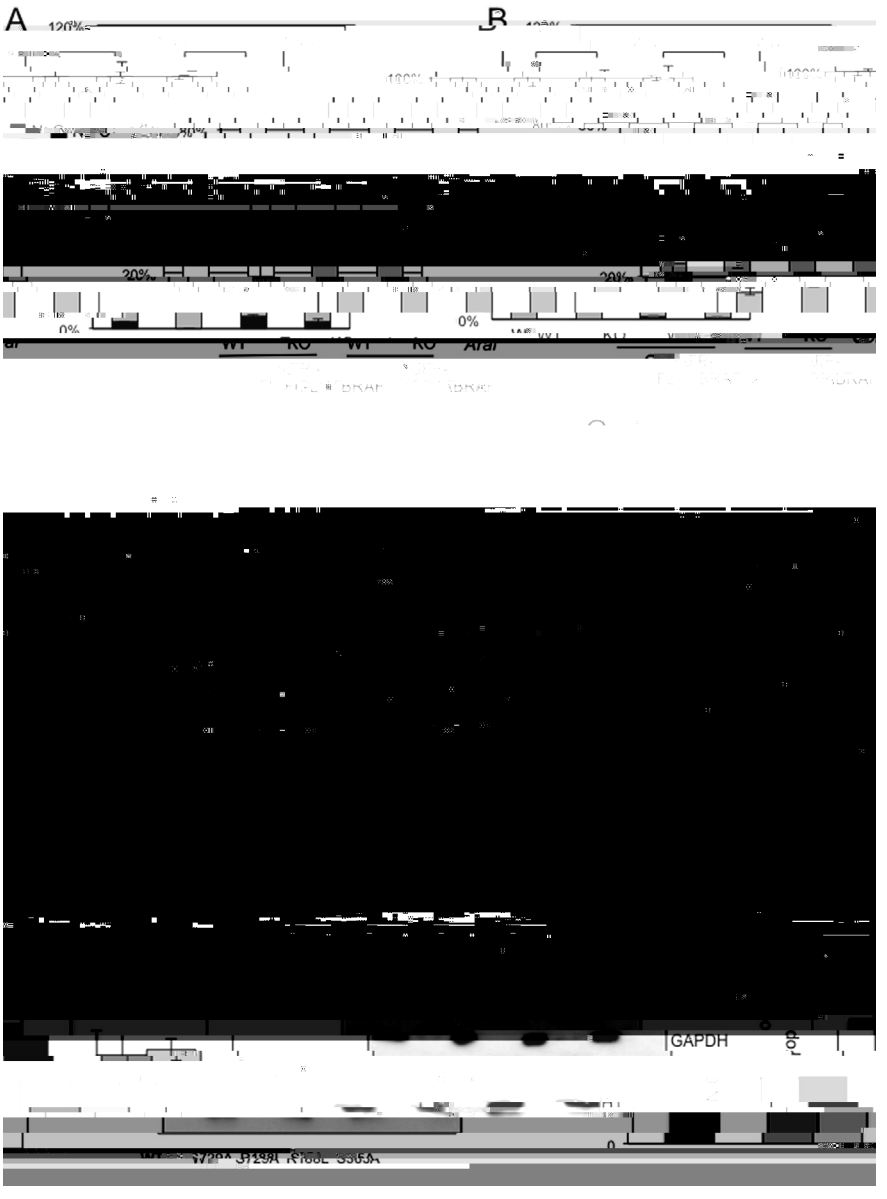

i . . Effect of CRAF, ARAF, ^{G12D}KRAS and 14-3-3 on GFP-BRAF localisation. (A) GFP-FL-^{WT}BRAF or GFP-ΔBRAF expression in Craf KO or wild-type MEFs followed by fluorescence microscopy quantitation. (B) GFP-FL-^{WT}BRAF or GFP-ΔBRAF in Araf KO or wild-type MEFs followed by fluorescence microscopy quantitation. (C) GFP-FL-^{WT}BRAF or GFP-ΔBRAF expression in wild-type or KRAS^{G12D} MEFs followed by fluorescence microscopy quantitation. (D) GFP-FL-BRAF with or without the R188L, S729A or S356A mutations or GFP-ΔBRAF expressed in NIH3T3 cells followed by fluorescence microscopy quantitation. For (A−D), cells were categorized as in Fig. 1B and bar charts show mean (n = 3) ± SEM. In (A−C), three different MEFs of each genotype were examined. (E) Cells from (D) were subjected to nuclear/cytoplasmic fractionation and western blots analysed with antibodies against GFP or with GAPDH or Histone H1 to confirm purity of fractions. Western blot data were quantified using Image J analysis to generate the N:C proportion indicated in the bar chart on the right. Data represent mean ± SEM (n = 3 for each vector).

https://doi.org/10.1016/j.heliyon.2018.e01065

on BRAF kinase activity [53] and therefore we investigated the link between downstream MEK-ERK activation and GFP-BRAF compartmentalisation. Using fractionation followed by immunoprecipitation and kinase cascade assays, we found that nuclear GFP-ΔBRAF had similar levels of kinase activity towards MEK-ERK as cytoplasmic GFP-ΔBRAF (Fig. 7A) and could bind to phosphorylated and non-phosphorylated forms of MEK and ERK (Fig. 7B). As a control, analysis of GFP alone showed negligible kinase activity and no binding to phosphorylated or non-phosphorylated MEK/ERK (Fig. 7A, B).

We monitored the compartmentalisation of MEK and ERK following expression of GFP, GFP-ΔBRAF, GFP-FL-^{WT}BRAF and GFP-FL-^{VE}BRAF in NIH3T3 cells using fractionation. In all cases, non-phosphorylated MEK1/2 and ERK2 were predominantly cytoplasmic and this distribution was not noticeably different between samples (Fig. 7C). As expected from the data shown in Fig. 7B, monomeric GFP did not induce detectable MEK or ERK phosphorylation (Fig. 7C). In contrast, all

811. In,a

i . . Localisation of phosphorylated MEK and ERK. (A) Nuclear GFP-ΔBRAF has kinase activity towards the MEK-ERK pathway. NIH3T3 cells were transfected with vectors expressing GFP or GFP-ΔBRAF. Whole cell lysates were prepared from the GFP-transfected cells while nuclear/cytoplasmic fractions were prepared from the GFP-ΔBRAF transfected cells. GFP expression levels and purity of fractions are indicated by

i . . High Content Microscopy (HCM). (A) Localisation of BRAF-GFP using HCM. NIH3T3 cells expressing either GFP-ΔBRAF or GFP-FL-^{WT}BRAF were treated with LMB for 3 hours and then subjected to HCM analysis. GFP staining was categorised into one of three categories as indicated where N > C represents >1.5 class nuclear staining, N=C represents 1−1.5 class nuclear staining and N < C represents <1 class nuclear staining. Mean values ± SEM are shown. (B) Localisation of PP-ERK. NIH3T3 cells expressing GFP-FL-^{WT}BRAF or GFP-ΔBRAF were treated with LMB for 3 hours, immunostained for PP-ERK1/2 and subjected to HCM. Representative digital images are shown. Cells were sorted into bins as described in Materials andMethods. The data are population averages (in AFU) from 3 repeat experiments, each with duplicate adenovirus infections and 500−600 cells per infection. Correlation coefficients (r) were determined for each dataset, converted to Z scores and compared to generate the p value indicated. (C) Localisation of PP-MEK. NIH3T3 cells expressing GFP-FL-^{WT}BRAF or GFP-ΔBRAF were treated with LMB for 3 hours, immunostained for PP-MEK and analysed by HCM. Representative digital images are shown. Cells were sorted into bins as described in Materials andMethods. The data in the graph are population averages (in AFU) from 3 repeat experiments, each with duplicate adenovirus infections and 500−600 cells per infection. Correlation coefficients (r) were determined for each dataset, converted to Z scores and compared to generate the p value indicated.

. ic a in

An overwhelming body of evidence has shown that the BRAF protein kinase, in its inactive conformation, is located in the cytoplasm as part of a multiprotein complex

https://doi.org/10.1016/j.heliyon.2018.e01065

containing 14-3-3 adaptor/scaffold proteins and heat-shock protein chaperones [12].

are too large to transit to the nucleus by diffusion, while monomeric GFP at ~27KDa is able to transit by diffusion. Consistently, the accumulation of the larger KIAA1549-BRAF fusion protein (~102KDa) in the nucleus argues against a diffusion mechanism (Fig. 3C). However, our data also exclude a role of energy-dependent selective transport that relies on the classical NLS-dependent import mechanism in the nuclear import of ΔBRAF (Fig. 4). Therefore, the mode of nuclear import of ΔBRAF is currently not clear. The fact that ΔBRAF accumulates in the

importance of the BRSR and CR1 domain (Fig. 6). Although we did not detect a ca-

The authors declare no conflict of interest.

Supplementary content related to this article has been published online at https://doi.org/10.1016/j.heliyon.2018.e01065.

We thank Steve Keyse (University of Dundee) and Craig McArdle (University of Bristol) for critical reviewing of the manuscript. Craig McArdle also provided advice on HCM. We dedicate this manuscript to the memory of our friend and colleague CJ Caunt.

References

[1] K.E. Mercer, C.A. Pritchard, Raf proteins and cancer: B-Raf is identified as a mutational target, Biochim. Biophys. Acta 1653 (2003) 25–40.

[2] S.M. Storm, U. Brennscheidt, G. Sithanandam, U.R. Rapp, Raf oncogenes in carcinogenesis, Crit. Rev. Oncog. 2 (1990) 1–8.

[3] G. Daum, I. Eisenmann-Tappe, H.W. Fries, J. Troppmair, U.R. Rapp, The ins and outs of Raf kinases, Trends Biochem. Sci. 19 (1994) 474–480.

[4] M.C. Lawrence, A. Jivan, C. Shao, L. Duan, D. Goad, E. Zaganjor, et al., The roles of MAPKs in disease, Cell Res. 18 (2008) 436–442.

[5] T. Kamata, C. Pritchard, Mechanisms of aneuploidy induction by RAS and

[10] R. Ciampi, J.A. Knauf, R. Kerler, M. Gandhi, Z. Zhu, M.N. Nikiforova, et al., Oncogenic AKAP9-BRAF fusion is a novel mechanism of MAPK pathway activation in thyroid cancer, J. Clin. Invest. 115 (2005) 94−101.

[11] P.T. Wan, M.J. Garnett, S.M. Roe, S. Lee, D. Niculescu-Duvaz, V.M. Good, et al., Mechanism of activation of the RAF-ERK signaling pathway by oncogenic mutations of B-RAF, Cell 116 (2004) 855−867.

[12] C. Wellbrock, M. Karasarides, R. Marais, The RAF proteins take centre stage, Nat. Rev. Mol. Cell Biol. 5 (2004) 875−885.

[13] L.O. Murphy, J. Blenis, MAPK signal specificity: the right place at the right time, Trends Biochem. Sci. 31 (2006) 268−275.

[14] S. Yoon, R. Seger, The extracellular signal-regulated kinase: multiple substrates regulate diverse cellular functions, Growth Factors 24 (2006) 21−44.

[15] L.O. Murphy, S. Smith, R.H. Chen, D.C. Fingar, J. Blenis, Molecular interpretation of ERK signal duration by immediate early gene products, Nat. Cell Biol. 4 (2002) 556−564.

[16] J. Pouyssegur, P. Lenormand, Fidelity and spatio-temporal control in MAP kinase (ERKs) signalling, Eur. J. Biochem. 270 (2003) 3291−3299.

[17] M. Adachi, M. Fukuda, E. Nishida, Two co-existing mechanisms for nuclear import of MAP kinase: passive diffusion of a monomer and active transport of ɑ dimer,1999002)

MAPK activation and neosynthesis of nuclear anchoring proteins, J. Cell Biol. 142 (1998) 625–633.

[23] C.J. Caunt, C.A. McArdle, ERK phosphorylation and nuclear accumulation:

fusion gene defines the majority of pilocytic astrocytomas, Cancer Res. 68 (2008) 8673−8677.

[34] C.J. Caunt, A.M. Kidger, S.M. Keyse, Visualizing and quantitating the spatio-temporal regulation of Ras/ERK signaling by dual-specificity mitogen-activated protein phosphatases (MKPs), Methods Mol. Biol. 1447 (2016) 197−215.

[35] K. Mercer, S. Giblett, A. Oakden, J. Brown, R. Marais, C. Pritchard, A-Raf and Raf-1 work together to influence transient ERK phosphorylation and Gl/S cell cycle progression, Oncogene 24 (2005) 5207−5217.

[36]

[43] C.J. Caunt, S.P. Armstrong, C.A. McArdle, Using high-content microscopy to study gonadotrophin-releasing hormone regulation of ERK, Methods Mol. Biol. 661 (2010) 507−524.

[44] C. Noble, K. Mercer, J. Hussain, L. Carragher, S. Giblett, R. Hayward, et al., CRAF autophosphorylation of serine 621 is required to prevent its proteasome-mediated degradation, Mol. Cell 31 (2008) 862−872.

[45] N.M. Seibel, J. Eljouni, M.M. Nalaskowski, W. Hampe, Nuclear localization of enhanced green fluorescent protein homomultimers, Anal. Biochem. 368 (2007) 95−99.

[46] M. Eilers, D. Picard, K.R. Yamamoto, J.M. Bishop, Chimaeras of myc oncoprotein and steroid receptors cause hormone-dependent transformation of cells, Nature 340 (1989) 66−68.

[47]

[54] C. de la Cova, I. Greenwald, SEL-10/Fbw7-dependent negative feedback regulation of LIN-45/Braf signaling in C. elegans via a conserved phosphodegron, Genes Dev. 26 (2012) 2524−2535.

[55] M.A. Hernandez, B. Patel, F. Hey, S. Giblett, H. Davis, C. Pritchard, Regulation of BRAF protein stability by a negative feedback loop involving the MEK-ERK pathway but not the FBXW7 tumour suppressor, Cell Signal. 28 (2016) 561−571.

[56] A. Kalmes, C. Hagemann, C.K. Weber, L. Wixler, T. Schuster, U.R. Rapp, Interaction between the protein kinase B-Raf and the alpha-subunit of the 11S proteasome regulator, Cancer Res. 58 (1998) 2986−2990.

[57] A. Ranganathan, M.N. Yazicioglu, M.H. Cobb, The nuclear localization of ERK2 occurs by mechanisms both independent of and dependent on energy, J. Biol. Chem. 281 (2006) 15645−15652.

[58] E. Zehorai, Z. Yao, A. Plotnikov, R. Seger, The subcellular localization of MEK and ERK-a novel nuclear translocation signal (NTS) paves a way to the nucleus, Mol. Cell. Endocrinol. 314 (2010) 213−220.

[59] H. Kosako, N. Yamaguchi, C. Aranami, M. Ushiyama, S. Kose, N. Imamoto,